JOURNAL OF BACTERIOLOGY, Nov. 2009, p. 6758–6768 Vol. 191, No. 21
0021-9193/09/$12.00 doi:10.1128/JB.00840-09

Uncovering the Protocatechuate 2,3-Cleavage Pathway Genes▽†

Daisuke Kasai,[1] Toshihiro Fujinami,[1] Tomokuni Abe,[2] Kohei Mase,[2]
Yoshihiro Katayama,[3] Masao Fukuda,[1] and Eiji Masai[1]*

Department of Bioengineering, Nagaoka University of Technology, Nagaoka, Niigata 940-2188,[1] Toyota Industries Corporation, Obu, Aichi 474-8601,[2] and Graduate School of Bio-Applications and Systems Engineering, Tokyo University of Agriculture and Technology, Koganei, Tokyo 184-8588,[3] Japan

Received 26 June 2009/Accepted 20 August 2009

***Paenibacillus* sp. (formerly *Bacillus macerans*) strain JJ-1b is able to grow on 4-hydroxybenzoate (4HB) as a sole source of carbon and energy and is known to degrade 4HB via the protocatechuate (PCA) 2,3-cleavage pathway. However, none of the genes involved in this pathway have been identified. In this study, we identified and characterized the JJ-1b genes for the 4HB catabolic pathway via the PCA 2,3-cleavage pathway, which consisted of *praR* and *praABEGFDCHI*. Based on the enzyme activities of cell extracts of *Escherichia coli* carrying *praI*, *praA*, *praH*, *praB*, *praC*, and *praD*, these genes were found to code for 4HB 3-hydroxylase, PCA 2,3-dioxygenase, 5-carboxy-2-hydroxymuconate-6-semialdehyde decarboxylase, 2-hydroxymuconate-6-semialdehyde dehydrogenase, 4-oxalocrotonate (OCA) tautomerase, and OCA decarboxylase, respectively, which are involved in the conversion of 4HB into 2-hydroxypenta-2,4-dienoate (HPD). The *praE*, *praF*, and *praG* gene products exhibited 45 to 61% amino acid sequence identity to the corresponding enzymes responsible for the catabolism of HPD to pyruvate and acetyl coenzyme A. The deduced amino acid sequence of *praR* showed similarity with those of IclR-type transcriptional regulators. Reverse transcription-PCR analysis revealed that *praABEGFDCHI* constitute an operon, and these genes were expressed during the growth of JJ-1b on 4HB and PCA. *praR-praABEGFDCHI* conferred the ability to grow on 4HB to *E. coli*, suggesting that *praEGF* were functional for the conversion of HPD to pyruvate and acetyl coenzyme A. A promoter analysis suggested that *praR* encodes a repressor of the *pra* operon.**

Protocatechuate (PCA) is one of the key intermediate metabolites in the microbial catabolic pathways for various aromatic compounds, including phthalates, hydroxybenzoates, and lignin-derived aromatic compounds such as vanillate and ferulate. It is known that the aromatic ring fission of PCA is catalyzed by one of the three distinct dioxygenases PCA 3,4-dioxygenase (26), PCA 4,5-dioxygenase (36, 41), and PCA 2,3-dioxygenase (7). In the PCA 3,4-cleavage pathway, PCA is converted into 2-carboxy-*cis*,*cis*-muconate by the reaction catalyzed by PCA 3,4-dioxygenase, and the catabolic pathway for its product (β-ketoadipate pathway) has been reported in many bacteria (24, 26). In the case of the PCA 4,5-cleavage pathway, PCA is cleaved by PCA 4,5-dioxygenase to yield 4-carboxy-2-hydroxymuconate-6-semialdehyde, and then the product is degraded to 2-pyrone-4,6-dicarboxylate, 4-oxalomesaconate, and 4-carboxy-4-hydroxy-2-oxoadipate before entering the Krebs cycle (36). The genes and enzymes involved in this pathway have been recently characterized for several bacteria, such as *Sphingobium* (*Sphingomonas*) (36), *Comamonas* (47), *Pseudomonas* (35), and *Arthrobacter* (13) strains. On the other hand, no genetic information on the PCA 2,3-cleavage pathway has been reported since the finding of this pathway in some bacilli (7, 8).

In 1979, Crawford et al. reported the PCA 2,3-cleavage pathway of a 4-hydroxybenzoate (4HB) degrader, *Paenibacillus* sp. (formerly *Bacillus macerans*) strain JJ-1b, which was isolated from a 50°C hot spring (9). In this pathway, PCA is initially transformed to 5-carboxy-2-hydroxymuconate-6-semialdehyde (5CHMS) by PCA 2,3-dioxygenase (Fig. 1A). 5CHMS was proposed to be subject to decarboxylation, resulting in the formation of 2-hydroxymuconate-6-semialdehyde (HMS), which is finally degraded to pyruvate and acetyl coenzyme A (9). Among these pathway enzymes, only the PCA 2,3-dioxygenase was purified and characterized in 1993 (64); however, all the genes responsible for the PCA 2,3-cleavage pathway have not yet been identified.

In the present study, we identified and characterized the 4HB catabolic gene (*pra* gene) cluster, including the PCA 2,3-cleavage pathway genes, from *Paenibacillus* sp. strain JJ-1b. This is the first report on the identification and characterization of the PCA 2,3-cleavage pathway genes.

MATERIALS AND METHODS

Bacterial strains, plasmids, and culture conditions. The bacterial strains and plasmids used in this study are listed in Table 1. *Paenibacillus* sp. strain JJ-1b was grown in Luria-Bertani (LB) medium or in W minimal salt medium (44) containing 10 mM 4HB, 10 mM PCA, or 10 mM succinate at 37°C. *Escherichia coli* strains were grown in LB medium at 30°C or 37°C. For cultures of *E. coli* cells carrying the ampicillin (Ap) resistance marker, the media were supplemented with 100 mg of Ap/liter.

Cloning of the *pra* genes. The E2GF and E2GR primer set (see Table S1 in the supplemental material) was used to amplify an aldehyde dehydrogenase gene sequence in JJ-1b. A 563-bp PCR-amplified fragment was used for colony hybridization as a probe to isolate the PCA 2,3-cleavage pathway genes from JJ-1b gene libraries, which were constructed using charomid 9-36 (50) with HindIII digests of the JJ-1b total DNA. The flanking sequences of the 3.4-kb HindIII fragment of pCH221 were obtained by using the 1.0-kb HindIII-KpnI fragment and the 1.0-kb XbaI-HindIII fragment as probes as shown in Fig. 1B. Colony and

* Corresponding author. Mailing address: Department of Bioengineering, Nagaoka University of Technology, Nagaoka, Niigata 940-2188, Japan. Phone and fax: 81-258-47-9428. E-mail: emasai@vos.nagaokaut.ac.jp.

† Supplemental material for this article may be found at http://jb.asm.org/.

▽ Published ahead of print on 28 August 2009.

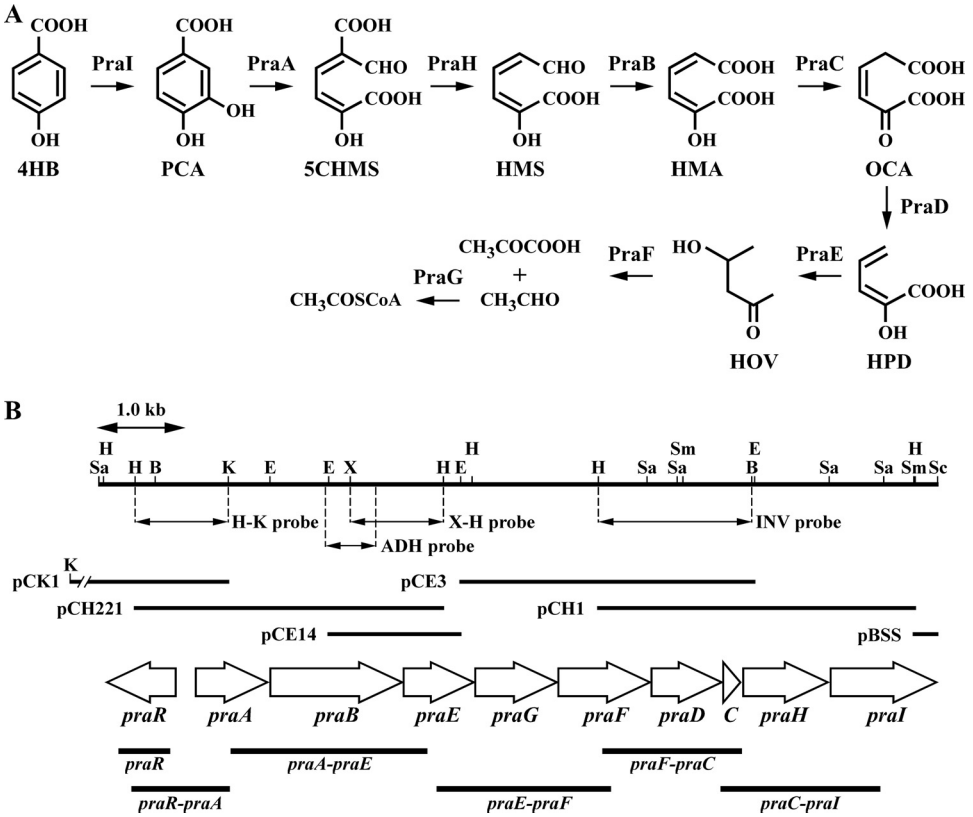

FIG. 1. Catabolic pathway of 4HB in *Paenibacillus* strain sp. JJ-1b (A) and organization of the *pra* gene cluster (B). (A) PraI, 4HB 3-hydroxylase; PraA, PCA 2,3-dioxygenase; PraH, 5CHMS decarboxylase; PraB, HMS dehydrogenase; PraC, OCA tautomerase; PraD, OCA decarboxylase; PraE, HPD hydratase; PraF, HOV aldolase; and PraG, acetaldehyde dehydrogenase (acylating). (B) Open arrows indicate the sizes, locations, and transcriptional directions of ORFs. The locations of the cloned DNA fragments are indicated above the arrows representing the ORFs. Double-headed arrows indicate the positions of probes used in library screening. Boldface bars below the gene cluster diagram indicate the locations of the amplified RT-PCR products shown in Fig. 6. Abbreviations for restriction enzymes: B, BamHI; E, EcoRI; H, HindIII; K, KpnI; Sa, SacI; Sc, ScaI; Sm, SmaI; and X, XbaI.

Southern hybridizations were performed using the digoxigenin system (Roche, Mannheim, Germany).

An inverse PCR was employed to amplify a DNA fragment containing the downstream region of pCE14 using the INVF and INVR primer set. Total DNA of JJ-1b was digested with BamHI and self-ligated, and then the ligation mixture was used as a template for the inverse PCR. The 1.7-kb HindIII-BamHI fragment of the amplified product was used for colony hybridization as a probe (INV probe shown in Fig. 1B) to isolate the 3.3-kb EcoRI fragment (pCE3) and the 3.5-kb HindIII fragment (pCH1) from gene libraries of JJ-1b as shown in Fig. 1B. The INV2F and INV2R primer set was designed for inverse PCR to amplify the region further downstream. Using BamHI-digested and self-ligated total DNA as a template, the DNA fragment was amplified. The 261-bp SmaI-ScaI fragment of the amplified region was cloned (pBSS) and sequenced. The nucleotide sequences of the primer sets are shown in Table S1 in the supplemental material.

DNA manipulations and nucleotide sequencing. DNA manipulations, including total DNA isolation, 16S rRNA gene amplification, construction of deletion derivatives, and nucleotide sequencing, were performed as described in previous studies (30, 54). Analysis of nucleotide sequences was performed using the MacVector software (MacVector, Inc., Cary, NC). Homology searches, pairwise alignment, and ClustalW multiple-sequence alignment were performed as described previously (1, 29). Analysis of the 16S rRNA gene was performed using the Ribosomal Database Project release 10.10 online server (6). A distance matrix and phylogenetic trees were constructed by using the neighbor-joining method (51) and were visualized with the FigTree program (version 1.2; http://tree.bio.ed.ac.uk/software/figtree/).

Construction of expression plasmids of the *pra* genes. *praA*, *praB*, *praC*, *praD*, *praH*, and *praI* were PCR amplified and subcloned into pT7Blue. In order to achieve ligation at the NdeI site of the expression vector, all of these genes were amplified with a forward primer designed to contain the NdeI site at its own ATG start codon (see Table S1 in the supplemental material). After the sequences were confirmed, each *praA*, *praB*, *praC*, *praH*, and *praI* fragment was ligated to an expression vector, pET21a(+), to form pETA23, pETB23, pETC23, pETH23, and pETI23, respectively. The *praD* fragment was ligated to pColdIV to construct pC4D23. To construct the *praCH* coexpression plasmid, pETCH23, the 1.8-kb EcoRI-HindIII fragment carrying *praH* was ligated into pETC23 digested with the same restriction enzymes.

Expression of the *pra* genes in *E. coli*. The expression plasmids were introduced into *E. coli* BL21(DE3) cells. BL21(DE3) cells harboring pETA23 were grown in 10 ml of LB medium containing 100 mg of Ap/liter at 37°C, and the cells harboring pETB23, pETC23, pETH23, pETI23, and pETCH23 were grown in the same medium at 30°C. Expression of *praA* was induced for 4 h by adding 0.1 mM isopropyl-β-D-thiogalactopyranoside (IPTG) when the absorbance of the culture at 600 nm (A_{600}) reached 0.5. Expression of *praB*, *praC*, *praH*, and *praI* and coexpression of *praC* and *praH* were induced by adding 1 mM IPTG, and then growth was continued for 4 h. BL21(DE3) cells harboring pC4D23 were grown in 10 ml LB medium containing Ap at 37°C until the A_{600} reached 0.5, and the culture was placed at 15°C for 30 min and cultivated again at 15°C for 24 h after the addition of 0.1 mM IPTG. Cells were harvested, resuspended in 50 mM Tris-HCl buffer (pH 7.3), broken with an ultrasonic disintegrator (UD-201; Tomy Seiko Co., Tokyo, Japan), and centrifuged at 15,000 × *g* for 15 min. The resulting supernatants were used as crude enzymes.

Enzyme assays. (i) PCA 2,3-dioxygenase. PCA 2,3-dioxygenase activity was assayed by measuring the substrate-dependent oxygen consumption rate. A 2-ml assay mixture contained 50 mM GTA buffer (pH 7.3) consisting of 50 mM 3,3-dimethylglutarate, 50 mM Tris, 50 mM 2-amino-2-methyl-1,3-propanediol, crude extract (2.5 μg of protein), and 100 μM PCA. The reaction mixture was incubated at 35°C, and the oxygen consumption rate was determined with an oxygen electrode (B-505; Iijima Electronics Manufacturing Co., Ltd., Aichi,

TABLE 1. Strains and plasmids used in this study

Strain or plasmid	Relevant characteristic(s)[a]	Source or reference
Strains		
Paenibacillus sp. strain JJ-1b	Wild type (ATCC 35889)	9
E. coli		
DH5	*supE44 hsdR17 recA1 endA1 gyrA96 thi-1 relA1*	21
DH5α	Δ(*lac*)U169 ϕ80 Δ(*lacZ*)M15 *hsdR17 endA1 gyrA96 recA1 relA1 supE44 thi-1*	21
BL21(DE3)	F^- *ompT hsdS*$_B$ (r_B^- m_B^-) *gal dcm* (DE3); T7 RNA polymerase gene under the control of the *lacUV*5 promoter	59
Plasmids		
Charomid 9-36	Ap^r cos	50
pBluescript II KS(+)	Cloning vector; Ap^r	56
pUC19	Cloning vector; Ap^r	65
pT7Blue	Cloning vector; Ap^r T7 promoter	Novagen
pET21a(+)	Expression vector; Ap^r T7 promoter	Novagen
pColdIV	Expression vector; Ap^r *cspA* promoter	Takara Bio
pQF50	Broad-host-range transcriptional fusion vector containing a promoterless *lacZ*; Ap^r	17
pPR9TT	Broad-host-range vector containing *lacZ* without ATG; Ap^r Cm^r	53
pPR9TZ	pPR9TT with a 3.6-kb SmaI-ScaI fragment containing *lacZ* from pQF50 replacing the 3.2-kb BamHI fragment	K. Takamura
pTE2G1	pT7Blue with a 563-bp PCR-amplified fragment containing *praB* internal region	This study
pCH221	Charomid 9-36 with a 3.4-kb HindIII fragment carrying *praA* and *praB*	This study
pCE14	Charomid 9-36 with a 1.5-kb EcoRI fragment	This study
pCK1	Charomid 9-36 with a 4.0-kb KpnI fragment	This study
pCE3	Charomid 9-36 with a 3.3-kb EcoRI fragment	This study
pCH1	Charomid 9-36 with a 3.5-kb HindIII fragment	This study
pBH3	KS(+) with a 3.4-kb HindIII fragment of pCH221	This study
pBE1F	KS(+) with a 1.5-kb EcoRI fragment of pCE14	This study
pBSK	KS(+) with a 1.4-kb SacI-KpnI fragment of pCK1	This study
pBE3F	KS(+) with a 3.3-kb EcoRI fragment of pCE3	This study
pBH4F	KS(+) with a 3.5-kb HindIII fragment of pCH1	This study
pTINVF	pT7Blue with a 3.3-kb PCR fragment generated by the INVF and INVR primer pair	This study
pBINV2H2	KS(+) with a 2.0-kb HindIII fragment of PCR fragment generated by the INV2F and INV2R primer pair	This study
pBBH	KS(+) with a 1.8-kb BamHI-HindIII fragment of pBH4F	This study
pBSS	KS(+) with a 0.3-kb SmaI-ScaI fragment of pBINV2H2	This study
pTN23	pT7Blue with a 603-bp PCR fragment generated by the praA-F and praA-R primer pair	This study
pTNB	pT7Blue with a 706-bp PCR fragment generated by the praB-F and praB-R primer pair	This study
pTCR	pT7Blue with a 392-bp PCR fragment generated by the praC-F and praC-R primer pair	This study
pTDF	pT7Blue with a 817-bp PCR fragment generated by the praD-F and praD-R primer pair	This study
pTH2	pT7Blue with a 155-bp PCR fragment generated by the praH-F and praH-R primer pair	This study
pTIR	pT7Blue with a 617-bp PCR fragment generated by the praI-F and praI-R primer pair	This study
pETA23	pET21a(+) with a 0.8-kb NdeI-EcoRI fragment carrying *praA*	This study
pETB23	pET21a(+) with a 1.9-kb NdeI-HindIII fragment carrying *praB*	This study
pETC23	pET21a(+) with a 0.4-kb NdeI-EcoRI fragment carrying *praC*	This study
pC4D23	pColdIV with a 0.8-kb NdeI-XhoI fragment carrying *praD*	This study
pETH23	pET21a(+) with a 1.9-kb NdeI-HindIII fragment carrying *praH*	This study
pETI23	pET21a(+) with a 1.4-kb NdeI-BamHI fragment carrying *praI*	This study
pETCH23	pET21a(+) with a 2.2-kb NdeI-HindIII fragment carrying *praC* and *praH*	This study
pBRI23	KS(+) with a 9.4-kb SacI-ScaI fragment carrying *pra* genes	This study
pPZAR	pPR9TZ with a 1.3-kb SacI-SacII fragment carrying *praR* and *praA* promoter region	This study
pPZA	pPR9TZ with a 0.6-kb PstI-SacII fragment carrying the *praA* promoter region	This study

[a] Ap^r and Cm^r, resistance to ampicillin and chloramphenicol, respectively.

Japan). One unit of enzyme activity was defined as the amount of enzyme that resulted in consumption of 1 μmol of O_2 per min at 35°C. Specific activity was expressed in units per milligram of protein. PCA 2,3-dioxygenase activity was also monitored using a DU-7500 spectrophotometer (Beckman Coulter, Fullerton, CA). The reaction mixture (final volume, 1 ml) containing 50 mM Tris-HCl buffer (pH 7.3), 50 μM PCA, and crude extract (2.5 μg of protein) was preincubated without the substrate for 1 min at 35°C, and then the reaction was started by adding PCA.

For gas chromatography-mass spectrometry (GC-MS) analysis, the reaction mixture was acidified with 6 N hydrochloric acid to pH 2 and extracted with ethyl acetate. The extract was trimethylsilylated with the TMSI-H reagent (hexamethyldisilazane-trimethylchlorosilane-pyridine [2:1:10]; GL Science Inc., Tokyo, Japan) according to the procedure recommended by the manufacturer. The resulting trimethylsilyl (TMS) derivatives were analyzed by GC-MS.

(ii) 5CHMS decarboxylase. 5CHMS decarboxylase activity was assayed spectrophotometrically by monitoring the production of HMS from 5CHMS using a preassay mixture that consisted of 50 μM PCA and crude PraA (2.5 μg of protein) in 50 mM Tris-HCl buffer (pH 7.3) in a total volume of 900 μl. The mixture was incubated for 1 min at 35°C. After the reaction was completed, crude PraH (10 μg of protein) was added in a final volume of 1 ml, and then the decrease in the absorbance at 350 nm and the increase in the absorbance at 375 nm were monitored at 35°C.

(iii) HMS dehydrogenase. HMS dehydrogenase activity was determined spectrophotometrically by monitoring the conversion of HMS to 2-hydroxymuconate

(HMA) using a preassay mixture that consisted of 1 mM PCA and crude PraA (4 μg of protein) in 50 mM Tris-HCl buffer (pH 7.3) in a total volume of 50 μl. The reaction mixture was incubated for 30 min at 35°C, and the increase in the absorbance at 375 nm due to the formation of HMS from PCA was monitored. After the reaction was completed, crude PraB (25 μg of protein) and 50 μM NAD^+ were added to the mixture. The reaction was carried out in a 1-ml reaction mixture at 35°C. For GC-MS analysis, the reaction mixture was acidified, extracted, and trimethylsilylated.

To determine the specific activity, 1 ml of reaction mixture containing 50 mM Tris-HCl buffer (pH 7.3), 50 μM HMS, crude PraB (25 μg of protein), 1.2 mM pyruvate, 1.0 U lactate dehydrogenase, and 500 μM $NAD(P)^+$ was incubated at 35°C, and the decrease in the absorbance at 375 nm was monitored. The specific activity was calculated from the initial rates by using a molar extinction coefficient of 35,000 M^{-1} cm^{-1} for HMS. One unit of HMS dehydrogenase activity was defined as the amount of enzyme that converted 1 μmol of HMS per minute under the assay conditions used.

(iv) OCA tautomerase. 4-Oxalocrotonate (OCA) tautomerase activity was determined spectrophotometrically by measuring the formation of OCA at 236 nm (25). The reaction was carried out in a 1-ml reaction mixture containing 50 mM Tris-HCl buffer (pH 7.3), 50 μM NAD^+, 50 μl of the PraA reaction mixture, crude PraB (25 μg of protein), and crude PraC (25 μg of protein) at 35°C.

(v) OCA decarboxylase. OCA decarboxylase activity was determined by measuring the production of 2-hydroxypenta-2,4-dienoate (HPD) by high-performance liquid chromatography (HPLC) (Acquity Ultra Performance LC; Waters, Milford, MA). The assay was performed by using a preassay mixture that consisted of 50 μl of the PraA reaction mixture, 50 μM NAD^+, crude PraB (25 μg of protein/ml), and crude PraC (25 μg of protein/ml) in 50 mM Tris-HCl buffer (pH 7.3) in a total volume of 990 μl. The reaction mixture was incubated for 30 min at 35°C; crude PraD (25 μg of protein) and 500 μM $MgSO_4$ were then added to the mixture to obtain a final volume of 1 ml. The reaction mixture was further incubated at 35°C for 10 min, and the enzyme reaction was stopped by addition of methanol (final concentration, 25%). The stopped reaction mixture was then subjected to HPLC (Acquity Ultra Performance LC; Waters, Milford, MA) analysis.

(vi) 4HB 3-hydroxylase. 4HB 3-hydroxylase activity was measured spectrophotometrically by monitoring the decrease in the absorbance at 340 nm derived from the consumption of NADH or NADPH at 35°C. The assay mixture (final volume, 1 ml) contained 50 mM Tris-HCl buffer (pH 8.0), 200 μM NAD(P)H, 500 μM EDTA, 10 μM flavin adenine dinucleotide (FAD), 1 mM 4HB, and crude PraI (200 μg of protein). The assay mixture was preincubated without the substrate for 1 min at 35°C, and the reaction was started by adding 4HB. The specific activity was calculated from the initial rates by using molar extinction coefficients of 6,600 and 5,070 M^{-1} cm^{-1} for NADH and NADPH, respectively (37). One unit of 4HB 3-hydroxylase activity was defined as the amount of enzyme that consumed 1 μmol of NADH or NADPH per minute under the assay conditions used.

For GC-MS analysis, the assay was carried out in a 1-ml reaction mixture containing 50 mM Tris-HCl buffer (pH 8.0), 1 mM NADH, 500 μM EDTA, 10 μM FAD, 100 μM 4HB, and crude PraI (200 μg of protein). After the reaction, the reaction mixture was acidified, extracted, trimethylsilylated, and analyzed by GC-MS.

RNA preparation and reverse transcription-PCR (RT-PCR) analysis. JJ-1b cells were grown in W minimal salt medium supplemented with 10 mM 4HB, PCA, or succinate at 37°C. When the A_{600} reached about 0.8, the cells were harvested by centrifugation at 5,000 × *g* at 4°C for 10 min. Total RNA was isolated with Isogen (Nippon Gene, Toyama, Japan) and then treated with DNase I (Takara Bio Inc.). Single-stranded cDNA was synthesized from 5.0 μg of total RNA by using PrimeScript reverse transcriptase (Takara Bio Inc.) with random primers in a 20-μl reaction mixture. PCR amplification was performed with a 1.0 μl of the cDNA mixture, specific primers (see Table S1 in the supplemental material), and Ex *Taq* DNA polymerase (Takara Bio Inc.). A control without reverse transcriptase was used for each reaction to verify the absence of genomic DNA contamination. PCR samples were electrophoresed on a 0.8% agarose gel and visualized with ethidium bromide.

Measurement of the promoter activity. The 1.3-kb SacI-SacII fragment carrying *praR* and the potential *pra* operon promoter was cloned into the promoter-probe vector pPR9TZ to obtain pPZAR. The 0.6-kb PstI-SacII fragment was also cloned into pPR9TZ to create pPZA carrying only the potential *pra* operon promoter. Expression of the *lacZ* reporter gene was determined by β-galactosidase (β-Gal) assays performed as follows. *E. coli* DH5α cells harboring pPZAR or pPZA were grown in 10 ml of LB medium either with or without 10 mM 4HB or PCA at 37°C. After 12 h, cells were harvested and resuspended in Z buffer, consisting of 50 mM sodium phosphate buffer (pH 7.0), 10 mM KCl, 1 mM $MgSO_4$, and 50 mM β-mercaptoethanol. Toluene treatment and β-Gal assays using *o*-nitrophenyl-β-D-galactopyranoside were performed as described by Miller (38). The values presented are the averages and standard deviations (error bars) from at least three independent experiments.

Analytical methods. The protein concentration was determined by the method of Bradford (5). The sizes of the proteins expressed in *E. coli* were examined by sodium dodecyl sulfate-12% polyacrylamide gel electrophoresis (SDS-PAGE). The proteins in the gels were stained with Coomassie brilliant blue R-250. To determine the N-terminal amino acid sequence, the crude extract was subjected to SDS-PAGE and electroblotted onto a polyvinylidene difluoride membrane (Bio-Rad, Hercules, CA). The enzyme band was cut out and analyzed on a Procise 494 HT protein sequencing system (Applied Biosystems, Foster City, CA). GC-MS analysis was performed with a model 5971A instrument equipped with an Ultra-2 capillary column (50 m by 0.2 mm; Agilent Technologies Co., Palo Alto, CA). The analytical conditions were the same as those described previously (29). HPLC analysis was performed with an Acquity Ultra Performance LC (Waters) equipped with a TSKgel ODS-140HTP column (2.1 by 100 mm; Tosoh, Tokyo, Japan). The mobile phase was 1% (vol/vol) acetonitrile in water containing 0.1% (vol/vol) phosphoric acid, and the flow rate was 0.5 ml/min. HMA, OCA, and HPD were detected at 303, 228, and 272 nm, respectively.

Nucleotide sequence accession numbers. The nucleotide sequence reported in this paper has been deposited in the DDBJ, EMBL, and GenBank nucleotide sequence databases under accession numbers AB505863 and AB505864.

RESULTS

16S rRNA gene analysis of JJ-1b. The nucleotide sequence of the 16S rRNA gene of JJ-1b showed significant similarity to those of *Paenibacillus validus* 197 (99.2% identity, 1,456-bp overlap; accession no. EU730934), *Paenibacillus* sp. strain Ao3 (97.0% identity, 1,515-bp overlap; EF208754), *Paenibacillus* sp. strain HM1 (96.9% identity, 1,515-bp overlap; AY283261), and *Paenibacillus validus* JCM 9077 (96.8% identity, 1,487-bp overlap; AB073203). Accordingly, we propose to rename *Bacillus macerans* JJ-1b as *Paenibacillus* sp. strain JJ-1b.

Cloning and nucleotide sequences of the PCA 2,3-cleavage pathway genes. In order to isolate the PCA 2,3-cleavage pathway genes from JJ-1b, we first attempted to isolate the HMS dehydrogenase gene. Based on the sequence similarity among putative 5-carboxymethyl-2-hydroxymuconate semialdehyde dehydrogenases from *Bacillus cereus* NVH 391-98 (ABS21296) and *Geobacillus kaustophilus* HTA426 (BAD77313) and a putative aldehyde dehydrogenase (AAU25432) from *Bacillus licheniformis* ATCC 14580, a primer set (E2GF and E2GR) was designed and used to amplify a 563-bp DNA fragment from total DNA of JJ-1b. The nucleotide sequence of this fragment showed 67% identity with that of AAU25432. The resulting PCR fragment was then used as a probe to screen a JJ-1b genomic library, and a positive clone, pCH221, carrying the 3.4-kb HindIII fragment was obtained. The nucleotide sequence of the 3.4-kb HindIII fragment was determined, and two open reading frames (ORFs), named *praA* and *praB*, were found. The homology search revealed that the *praA* and *praB* gene products showed similarity with homoprotocatechuate 2,3-dioxygenases and HMS dehydrogenases, respectively (Table 2). To acquire the flanking region of the 3.4-kb HindIII fragment, colony hybridization and inverse PCR were performed. As a result, five clones, pCK1, pCE14, pCE3, pCH1, and pBSS, were obtained (Fig. 1B). Using these clones, the nucleotide sequence of the 9,354-bp region was determined. In this region, 10 ORFs containing *praA* and *praB* were found. Nine of these ORFs are transcribed in the same direction; the exception is *praR*, which appeared to encode a putative tran-

TABLE 2. Identification of *pra* gene functions

Gene	Deduced molecular mass, Da (no. of amino acid residues)	Representative homolog	Identity (%)[a]	Accession no.
praR	28,947 (258)	IclR-type transcriptional regulator from *Bacillus licheniformis* ATCC 14580	49	AAU25433
		IclR-type transcriptional regulator (PcaU) from *Acinetobacter baylyi* ADP1	25	AAC37157
praA	29,636 (266)	Hypothetical protein from *B. licheniformis* ATCC 14580	53	AAU25429
		HPCA 2,3-dioxygenase (HpaD) from *Pseudomonas* sp. strain DJ-12	29	AAL28115
		HPCA 2,3-dioxygenase (HpaD) from *Burkholderia xenovorans* LB400	28	ABE33954
		HPCA 2,3-dioxygenase (HpcB) from *Escherichia coli* C	26	CAA38985
praB	53,188 (486)	Aldehyde dehydrogenase from *B. licheniformis* ATCC 14580	74	AAU25432
		HMS dehydrogenase (NahI) from *Pseudomonas putida* G7 (NAH7)	55	BAE92168
		HMS dehydrogenase (XylG) from *P. putida* mt-2 (pWW0)	54	AAA26053
praE	27,687 (260)	HPD hydratase (BphH) from *B. xenovorans* LB400	52	ABE37051
		HPD hydratase (NbaH) from *Pseudomonas fluorescens* KU-7	45	BAC65306
praG	31,466 (294)	Acetaldehyde dehydrogenase (NahO) from *Bacillus* sp. strain JF8	61	BAD08310
		Acetaldehyde dehydrogenase (NbaJ) from *P. fluorescens* KU-7	53	BAC65307
praF	36,116 (337)	HOV aldolase (NahM) from *Bacillus* sp. strain JF8	58	BAD08311
		HOV aldolase (XylK) from *P. putida* mt-2 (pWW0)	51	AAA25692
praD	28,125 (260)	Putative OCA decarboxylase from *B. licheniformis* ATCC 14580	64	AAU25431
		OCA decarboxylase (XylI) from *P. putida* mt-2 (pWW0)	46	AAA25693
praC	7,012 (63)	Putative OCA tautomerase from *B. licheniformis* ATCC 14580	64	AAU25430
		OCA tautomerase (DmpI) from *Pseudomonas* sp. strain CF600	49	CAA43229
praH	35,570 (313)	Putative decarboxylase from *B. licheniformis* ATCC 14580	58	AAU25434
		ACMS decarboxylase (NbaD) from *P. fluorescens* KU-7	24	BAC65312
praI	44,262 (394)	Putative 4HB 3-hydroxylase from *B. licheniformis* ATCC 14580	66	AAU25427
		4HB 3-hydroxylase (PobA) from *Arthrobacter* sp. strain ATCC 51369	45	BAE46572

[a] Percent identity obtained by aligning the deduced amino acid sequences by use of the EMBOSS alignment tool.

scriptional regulator. The gene products of *praE*, *praG*, *praF*, *praD*, *praC*, and *praI* showed similarity with HPD hydratase, acetaldehyde dehydrogenase (acylating), 4-hydroxy-2-oxovalerate (HOV) aldolase, OCA decarboxylase, OCA tautomerase, and 4HB 3-hydroxylase, respectively (Table 2). PraH showed similarity with 2-amino-3-carboxymuconate-6-semialdehyde (ACMS) decarboxylase (NbaD) from *Pseudomonas fluorescens* KU-7 (BAC65312), suggesting that *praH* encodes 5CHMS decarboxylase (Table 2).

Identification of PraA as PCA 2,3-dioxygenase. The *praA* gene was expressed in *E. coli* harboring pETA23, which carries *praA* in pET21a(+). Production of a 31-kDa protein in *E. coli* BL21(DE3) cells harboring pETA23 was observed by SDS-PAGE (see Fig. S1 in the supplemental material). Absorption spectral analysis revealed that PCA (λ_{max} = 254 and 290 nm) was converted by crude PraA into a product having a spectrum with a maximum at 350 nm (Fig. 2A). This spectrum is characteristic of 5CHMS (9). Therefore, it was strongly suggested that *praA* encodes PCA 2,3-dioxygenase. The specific activity of crude PraA toward PCA was determined to be 32.9 ± 1.8 U/mg. When the reaction mixture was incubated for 20 min, a decrease in the absorbance at 350 nm and an increase in the absorbance at 375 nm were observed (Fig. 2B). According to previous studies (9, 52), this spectrum is characteristic of HMS.

The PraA reaction mixture was analyzed by GC-MS. After 10 min of reaction, compound I, with a retention time of 18.5 min, was produced (see Fig. S2C in the supplemental material). The weight of the molecular ion of compound I (*m/z* 286) corresponded to that of TMS derivative of HMS. The major fragments at *m/z* 271, 257, 197, and 169 corresponded to M-CH_3, M-CHO, M-OTMS, and M-COOTMS, respectively (see Fig. S2D in the supplemental material). These results indicated that HMS was formed from PCA by the consecutive reactions of 2,3-ring cleavage and spontaneous decarboxylation. The accumulation of 5CHMS was not observed under these conditions, suggesting that 5CHMS was converted to HMS during the extraction and/or analysis process.

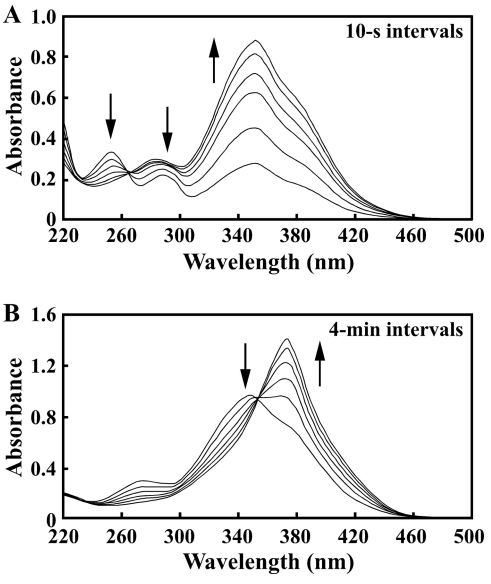

FIG. 2. Conversion of PCA to 5CHMS catalyzed by PraA. (A) The reaction mixture contained 50 mM Tris-HCl buffer (pH 7.3), 50 μM PCA, and crude PraA (2.5 μg of protein), and it was incubated at 35°C in a final volume of 1 ml. UV-visible spectra were recorded at intervals of 10 s. (B) The reaction mixture was the same as described above, but UV-visible spectra were recorded at intervals of 4 min.

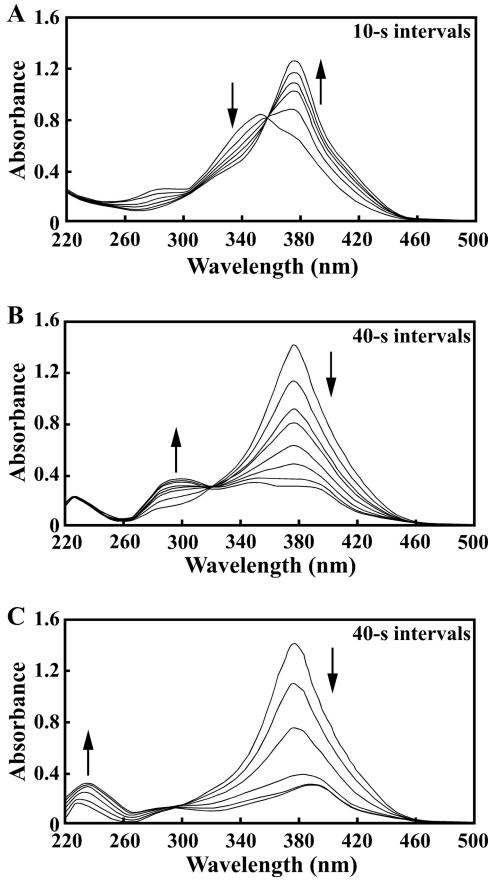

FIG. 3. Spectral changes associated with the transformations of 5CHMS to HMS (A), HMS to HMA (B), and HMS to OCA (C). (A) The reaction mixture contained 50 mM Tris-HCl buffer (pH 7.3), 50 μM PCA, crude PraA (2.5 μg of protein/ml), and crude PraH (10 μg of protein/ml). (B) The reaction mixture contained 50 mM Tris-HCl buffer (pH 7.3), 50 μM HMS, 50 μM NAD^+, and crude PraB (25 μg of protein/ml). (C) The reaction mixture contained 50 mM Tris-HCl buffer (pH 7.3), 50 μM HMS, 50 μM NAD^+, crude PraB (25 μg of protein/ml), and crude PraC (25 μg of protein/ml). UV-visible spectra were recorded at intervals of 10 s (A) and 40 s (B and C).

Identification of PraH as 5CHMS decarboxylase. The nucleotide sequence analysis predicted the presence of two consecutive ATG codons, which are possible *praH* start codons. The N-terminal amino acid sequence of PraH produced in *E. coli* harboring pETCH23, which carries *praCH*, was determined to be MYDVH; therefore, the second methionine was chosen as the start codon of *praH* to construct the *praH* expression plasmid, pETH23. SDS-PAGE analysis indicated the production of a 34-kDa protein in *E. coli* BL21(DE3) harboring pETH23 (see Fig. S1 in the supplemental material). 5CHMS produced from 50 μM PCA by the incubation with crude PraA was reacted with crude PraH. As shown in Fig. 3A, 5CHMS (λ_{max} = 350 nm) was converted into a product having a spectrum with a maximum at 375 nm after 1 min. On the other hand, 5CHMS was never degraded under the same conditions without PraH (data not shown). These results strongly suggested that *praH* encodes 5CHMS decarboxylase.

Characterization of the *praB*, *praC*, and *praD* gene products. The *praB*, *praC*, and *praD* genes were expressed in *E. coli* BL21(DE3) cells harboring pETB23, pETC23, and pC4D23, respectively. In SDS-PAGE analysis, the molecular masses of the products of *praB*, *praC*, and *praD* were estimated to be 58, 6, and 31 kDa, respectively (see Fig. S1 in the supplemental material).

The HMS dehydrogenase activity was assayed with crude PraB in the presence of 50 μM HMS, which was produced by the reaction catalyzed by PraA and spontaneous decarboxylation. The activity of crude PraB for HMS in the presence of NAD^+ (1.19 ± 0.07 U/mg of protein) was about 11 times higher than that achieved with $NADP^+$ (0.113 ± 0.009 U/mg of protein), indicating that PraB is highly specific for NAD^+. Absorption spectral analysis revealed that HMS (λ_{max} = 375 nm) was converted into a product having a spectrum with a maximum at 295 nm (Fig. 3B). This spectrum is characteristic of HMA (25, 52). When the reaction mixture was analyzed by GC-MS, the abundance of the TMS derivative of HMS decreased significantly at 5 min, and the accumulation of compound II with a retention time of 26.5 min was observed (see Fig. S3B and C in the supplemental material). The weight of the molecular ion of compound II (*m*/*z* 374) corresponded to that of the TMS derivative of HMA (see Fig. S3D in the supplemental material). These observations indicated that *praB* encodes HMS dehydrogenase.

During the transformation of HMS to HMA by the reaction catalyzed by PraB, crude PraC was added to the reaction mixture to allow the sequential reaction to occur. Absorption spectral analysis revealed that HMS was converted into a product having a spectrum with a maximum at 236 nm (Fig. 3C). This spectrum is characteristic of OCA (25); thus, HMA seemed to be converted to OCA by a tautomerization catalyzed by PraC.

Crude PraD was added to the PraC reaction mixture. When the mixture was analyzed by HPLC immediately after the start of the reaction, peaks with retention times of 0.89 and 2.50 min were observed (Fig. 4A to C). These peaks showed a spectrum with maxima at 228 and 303 nm, respectively. Therefore, these peaks appeared to be OCA and HMA, respectively, that were formed by keto-enol tautomerization. After 10 min of incubation, a product having a spectrum with a maximum at 272 nm was formed in significant amounts with a retention time of 6.03 min (Fig. 4D to F). Since the absorption maximum at 272 nm at pH 2.0 is characteristic of HPD (52), it was strongly suggested that this compound was HPD. Harayama and coworkers reported that OCA but not HMA was the substrate for OCA decarboxylase (25). Therefore, PraD appeared to catalyze the decarboxylation of OCA to produce HPD.

Identification of PraI as 4HB 3-hydroxylase. The *praI* gene was expressed in *E. coli* BL21(DE3) cells harboring pETI23. In SDS-PAGE analysis, the molecular mass of the *praI* product was estimated to be 41 kDa (see Fig. S1 in the supplemental material). The specific activities of crude PraI for 4HB in the presence of NADH and NADPH were determined to be 0.47 ± 0.01 and 0.36 ± 0.03 U/mg, respectively. These results indicated that PraI is able to utilize both NADH and NADPH as cofactors. GC-MS analysis of the PraI reaction mixture showed the disappearance of 4HB, and the formation of a compound with a retention time of 26.6 min was observed (Fig. 5). This compound was identified as PCA based on the comparison of retention times and mass fragmentation patterns

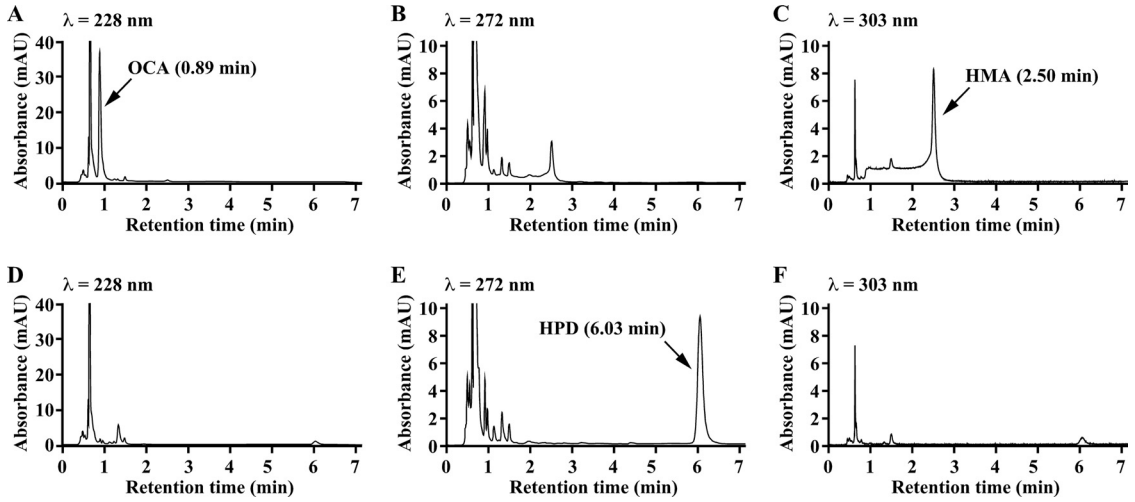

FIG. 4. HPLC chromatograms of the reaction product from OCA catalyzed by PraD. The reaction mixture contained the PraC reaction mixture, 500 μM $MgSO_4$, and crude PraD (25 μg of protein/ml) in 50 mM Tris-HCl buffer (pH 7.3) in a total volume of 1 ml. The PraC reaction mixture was prepared as described in Materials and Methods. The reaction mixtures were analyzed by HPLC at the start (A to C) and after 10 min (D to F) of incubation. Compounds were monitored at 228 nm (A and D), 272 nm (B and E), and 303 nm (C and F).

with those of authentic PCA (data not shown). Thus, *praI* was concluded to encode 4HB 3-hydroxylase.

***E. coli* acquires the ability to grow on 4HB by introduction of the *pra* gene cluster.** To test whether or not *pra* genes confer the ability to grow on 4HB to *E. coli*, DNA fragments derived from pBSK, pBH3, pBE1F, pBE3F, pBH4F, and pBSS were ligated into pBluescript II KS(+) as shown in Fig. S4 in the supplemental material. The resulting plasmid, pBRI23 carrying *praR-praABEGFDCHI*, was introduced into *E. coli* BL21(DE3) cells, and then the transformant was inoculated on M9 minimal salt medium containing 10 mM 4HB instead of glucose as the sole carbon source. The transformant obtained the ability to grow on 4HB within 10 days (see Fig. S4 in the supplemental material). This implies that *praR-praABEGFDCHI* is the complete gene set for the conversion of 4HB into pyruvate and acetyl coenzyme A.

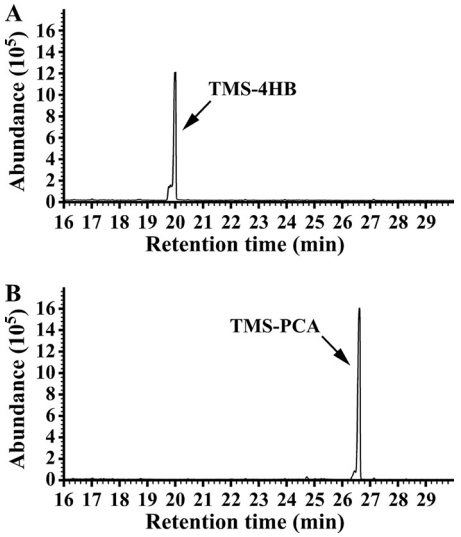

FIG. 5. Conversion of 4HB to PCA catalyzed by PraI. The reaction mixture contained 50 mM Tris-HCl buffer (pH 8.0), 1 mM NADH, 500 μM EDTA, 10 μM FAD, 100 μM 4HB, and crude PraI (200 μg of protein/ml). Gas chromatograms of TMS derivatives of the reaction products at the start (A) and after 10 min (B) of incubation are shown.

RT-PCR analysis of the *pra* genes. To define the operon structure of the *pra* genes, RT-PCR analysis was carried out with total RNA harvested from JJ-1b cells grown on 4HB or PCA. RT-PCR amplification products of the expected sizes were detected for genes *praA-praE*, *praE-praF*, *praF-praC*, *praC-praI*, and *praR* (Fig. 6A and B). However, no transcript between *praR* and *praA* was observed. These results suggested that *praABEGFDCHI* are organized in the same transcriptional unit, whereas *praR* is transcribed separately. As shown in Fig. 6C, amplification products for the *pra* catabolic genes were not evident when RNA from succinate-grown cells was used. This indicates that the growth of JJ-1b on 4HB and PCA leads to an increase in the transcription of the *pra* catabolic operon.

Transcriptional regulation of the *pra* operon. PraR is similar in sequence to transcriptional regulators belonging to the IclR family from *B. licheniformis* ATCC 14580 (AAU25433) and *Acinetobacter baylyi* ADP1 (PcaU; AAC37157) (Table 2). To investigate whether PraR plays a role in the transcriptional regulation of *pra* genes, the level of expression of the *praR-praA′-lacZ* fusion in *E. coli* DH5α cells harboring pPZAR and exposed to 4HB or PCA was examined. β-Gal activity was increased 19-fold and 12-fold in the presence of 4HB and PCA, respectively (Fig. 7). These results suggested that both 4HB and PCA acted as inducers for the *pra* catabolic operon. *E. coli* cells harboring pPZA, which includes a *praA* upstream region but not *praR*, showed constitutive expression (Fig. 7), suggesting that PraR is a transcriptional repressor of the *pra* operon.

DISCUSSION

In the present study, we identified the PCA 2,3-cleavage pathway genes involved in the 4HB catabolism of *Paenibacillus* sp. strain JJ-1b. The proposed 4HB catabolic pathway and the

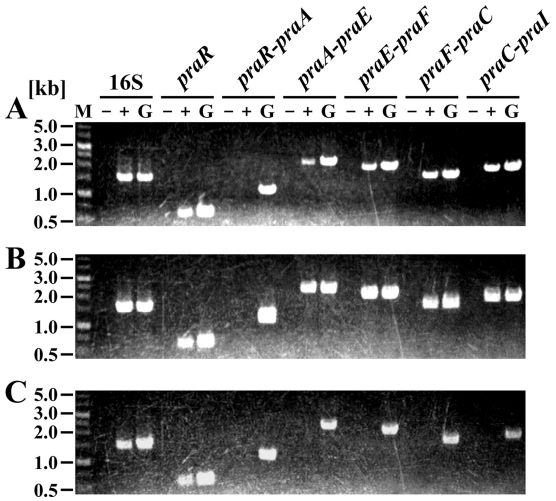

FIG. 6. RT-PCR analysis of the *pra* gene cluster in JJ-1b. Total RNA used for cDNA synthesis was isolated from JJ-1b cells grown on 4HB (A), PCA (B), and succinate (C). Agarose gel electrophoresis of RT-PCR assays with primers targeting *praR* (expected size, 572 bp), *praR-praA* (expected size, 1,092 bp), *praA-praE* (expected size, 2,190 bp), *praE-praF* (expected size, 1,940 bp), *praF-praC* (expected size, 1,553 bp), and *praC-praI* (expected size, 1,779 bp) are shown. Positions of primer pairs and primer sequences are indicated in Fig. 1B and in Table S1 in the supplemental material, respectively. Lane M, molecular weight markers; lanes + and −, RT-PCR with and without reverse transcriptase, respectively; lanes G, control PCR with the JJ-1b genomic DNA. RT-PCR of the 16S rRNA gene was used as a control to confirm equivalent quantities of template loading.

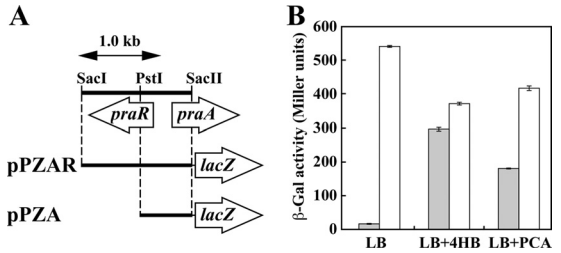

FIG. 7. Regulation of the *pra* operon promoter activity by PraR. (A) Schematic representation of pPZAR and pPZA. (B) Promoter activities of the *pra* operon were measured in *E. coli* cells harboring pPZAR (shaded bars) or pPZA (open bars). These cells were grown in LB medium with or without 10 mM 4HB or PCA. Each value is the average ± standard deviation (error bars) based on at least three independent experiments.

corresponding genes for the enzymes of JJ-1b are indicated in Fig. 1A.

4HB is transformed to PCA by the reaction catalyzed by PraI, which utilizes both NADH and NADPH as electron donors. 4HB 3-hydroxylases can be divided into two groups on the basis of the coenzyme specificity: (i) NADPH-specific and (ii) NAD(P)H-dependent 4HB 3-hydroxylases. A phylogenetic analysis of 4HB 3-hydroxylases indicated that NADPH-specific and NAD(P)H-dependent enzymes are located in the different branches (see Fig. S5A in the supplemental material). PraI forms a cluster with NAD(P)H-dependent enzymes. The deduced amino acid sequence alignment of PraI and NADPH-specific 4HB 3-hydroxylases indicated that Tyr38 and Arg42, which are essential for binding with NADPH (15, 16), are replaced by glutamate and threonine residues, respectively (see Fig. S5B in the supplemental material). These residues are highly conserved in the NAD(P)H-dependent 4HB 3-hydroxylases and are required for the recognition of NADH (15, 28).

PCA 2,3-dioxygenase had been previously purified and biochemically characterized (64), but the gene sequence has been unavailable. The *praA* gene product shares amino acid sequence similarity with extradiol dioxygenases. Extradiol dioxygenases have been divided into three families on the basis of amino acid sequence similarity (63). Type I extradiol dioxygenases belong to the vicinal oxygen superfamily, including a number of 2,3-dihydroxybiphenyl 1,2-dioxygenases (3, 27) and catechol 2,3-dioxygenases (40). Type II dioxygenases include several homoprotocatechuate 2,3-dioxygenases (49), the β subunit of PCA 4,5-dioxygenase (41, 47), gallate dioxygenase (30, 42), and 2-aminophenol 1,6-dioxygenase (61). Type III dioxygenases belong to the cupin superfamily, which includes enzymes such as the gentisate dioxygenase, homogentisate dioxygenase, and 1-hydroxy-2-naphthoate dioxygenase (12). These three types of enzymes have similar active sites and the same iron ligand, two histidines, and one glutamate (2-His-1-carboxylate structural motif), in spite of their different primary structures (31). As can be seen in the phylogenetic relationships of type II extradiol dioxygenases (see Fig. S6 in the supplemental material), PraA obviously belongs to the type II extradiol dioxygenase family and is closely related to a hypothetical protein (BL03909) of *B. licheniformis* ATCC 14580. However, the sequence of PraA formed a deep branch with those of the β subunit of PCA 4,5-dioxygenase, suggesting that they independently evolved from a common ancestor. Crystallographic studies revealed that the active site of the β subunit of PCA 4,5-dioxygenase (LigB) contains a nonheme iron coordinated by His12, His61, and Glu242, and His195 is thought to act as an active-site base to facilitate deprotonation of the hydroxyl group of the substrate (60). These amino acids are conserved among almost all the type II extradiol dioxygenases (14). The alignment of the deduced amino acid sequences of PraA and LigB revealed the presence of residues His11, His53, His180, and Glu227 of PraA, corresponding to His12, His61, His195, and Glu242, respectively, of LigB. These residues seemed to be involved in the roles described above.

When PCA was incubated with crude PraA, 5CHMS produced from PCA underwent spontaneous decarboxylation to HMS. However, no production of 5CHMS from PCA was observed in the reaction mixture containing the crude extract of JJ-1b (9). These facts suggested that 5CHMS decarboxylase encoded by *praH* plays a role in the decarboxylation of 5CHMS to HMS in JJ-1b cells. Based on the deduced amino acid sequence similarity, PraH seemed to be included in the metallo-dependent hydrolase (amidohydrolase_2) superfamily (33). This family includes ACMS decarboxylase from bacteria, animals, and humans (19, 39, 62); uracil-5-carboxylate decarboxylase of *Neurospora crassa* OR74A (57); the γ-resorcylate decarboxylase GraF from *Rhizobium* sp. strain MTP-10005 (66, 67); the 5-carboxyvanillate decarboxylase LigW (46); the biphenyl *meta*-cleavage compound hydrolase LigY (45); and the 4-oxalomesaconate hydratase LigJ (22) from *Sphingobium* sp. strain SYK-6. A phylogenetic analysis based on the amino acid sequences of the metallo-dependent hydrolase superfamily

clearly indicated that PraH belongs to this superfamily but does not form a cluster with the other known members (see Fig. S7 in the supplemental material). It has been indicated for ACMS decarboxylase from *P. fluorescens* (NbaD) that the active-site Zn ion is directly coordinated by His9, His11, His177, Asp294, and the water molecule which is hydrogen bonded with His228 (32, 34). These residues are essential for the ACMS decarboxylase activity. In the case of PraH, His5, His7, His173, His222, and Asp288 seemed to be involved in the coordination of the Zn ion.

praE, *praF*, and *praG* are similar to the genes for HPD hydratase, HOV aldolase, and acetaldehyde dehydrogenase, respectively. The corresponding genes were also found in the clusters that encode the aromatic ring cleavage pathways for 2-aminophenol (61), 2-nitrobenzoate (39), and catechol (23, 58). According to the sequence similarity, these gene products most likely have the same functions. The facts that *E. coli* carrying *praR-praABEGFDCHI* on a plasmid was able to grow on 4HB as the sole carbon source (see Fig. S4 in the supplemental material) and that the transcription of these genes is induced during 4HB catabolism (Fig. 6) support this notion.

Based on the sequence similarity, PraR belongs to the IclR family of transcriptional regulators, which includes PcaU and PcaR, activators of β-ketoadipate pathway genes in *Acinetobacter baylyi* ADP1 (10, 20) and *Pseudomonas putida* PRS2000 (48), respectively, PobR, an activator of the 4HB 3-hydroxylase gene, *pobA* from *A. baylyi* ADP1 (11), as well as HmgR, a repressor of the homogentisate catabolic pathway genes of *P. putida* U (2). It has been reported that PCA, β-ketoadipate, 4HB, and homogentisate act as inducers for the PcaU, PcaR, PobR, and HmgR regulatory systems, respectively. RT-PCR analysis and β-Gal assay of the *praA* promoter (Fig. 6 and 7) indicated that both 4HB and PCA are inducers of the *pra* catabolic operon. The promoter activity was constitutively observed, in the absence of *praR*, suggesting that *praR* codes for a repressor of the *pra* catabolic operon.

The gene organizations of the *pra* genes and the catechol *meta*-cleavage pathway genes on the TOL plasmid pWW0 of *P. putida* mt-2 (*xyl*) (18, 23), the naphthalene-catabolic plasmid NAH7 of *P. putida* G7 (*nah*) (58), and pVI150 of *Pseudomonas* sp. strain CF600 (*dmp*) (4, 43, 55) are almost identical, with the exception of the presence of *praH* and *praI* in the *pra* operon (Fig. 8). In the catechol *meta*-cleavage pathway gene clusters, the HMS hydrolase genes, *xylF*, *nahN*, and *dmpD*, are located between the HMS dehydrogenase genes (*xylG*, *nahI*, and *dmpC*) and the HPD hydratase genes (*xylJ*, *nahL*, and *dmpE*). However, the HMS hydrolase gene was missing in the *pra* gene cluster. Moreover, in the neighboring region of the *pra* gene cluster, the gene corresponding to *xylT* and *nahT*, which encode a chloroplast-type ferredoxin, was not observed.

In the *B. licheniformis* ATCC 14580 genome (CP000002), the genes related to *praH*, *praR*, *praB*, *praD*, *praC*, *praA*, and *praI* organize a gene cluster (Fig. 8). This cluster contains a gene encoding a putative benzoate transporter (BL03910), but the genes corresponding to *praE*, *praF*, and *praG* were absent. Recently, a draft genome sequence of *Geobacillus* sp. strain Y412MC61 has been reported (http://www.jgi.doe.gov/), and a gene cluster containing *praH*, *praR*, *praB*, *praE*, *praG*, *praF*, *praD*, *praC*, and *praA* orthologs was found (Fig. 8). This gene cluster has a complete set of the PCA 2,3-cleavage pathway genes except for the 4HB 3-hydroxylase gene. The presence of the *pra* gene cluster only in the genomes of bacilli suggested that the PCA 2,3-cleavage pathway genes might have evolved specifically in this particular group of bacteria.

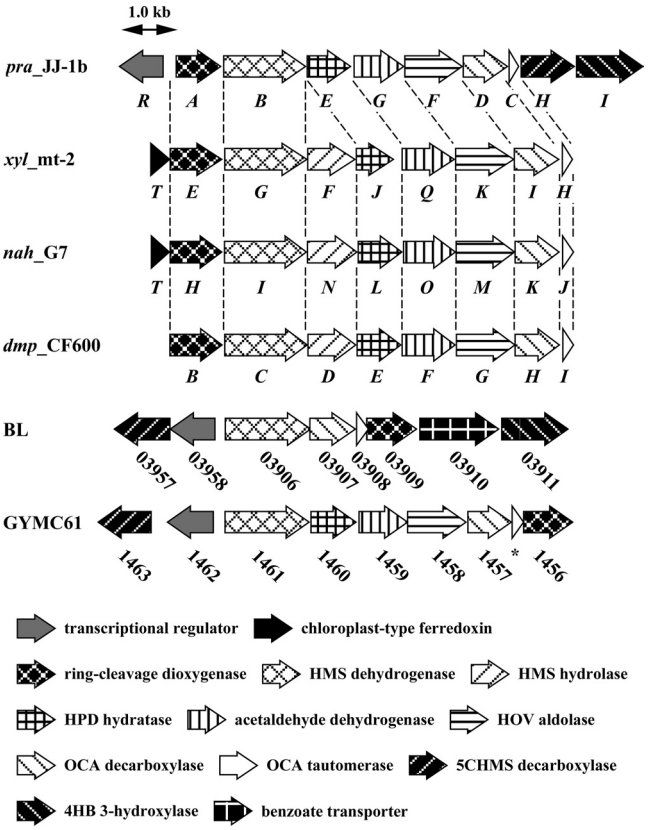

FIG. 8. Organizations of the gene clusters involved in the PCA 2,3-cleavage pathway and the catechol *meta*-cleavage pathway. *pra*_JJ-1b, the *pra* gene cluster in JJ-1b; *xyl*_mt-2, the *xyl* gene cluster in pWW0 of *P. putida* mt-2 (AJ344068); *nah*_G7, the *nah* gene cluster in NAH7 of *P. putida* G7 (AB237655); *dmp*_CF600, the *dmp* gene cluster in pVI150 of *Pseudomonas* sp. strain CF600 (M33263, X52805, and X60835); BL, the putative PCA 2,3-cleavage pathway gene cluster of *B. licheniformis* ATCC 14580 (CP000002); GYMC61, the putative PCA 2,3-cleavage pathway gene cluster of *Geobacillus* sp. strain Y412MC61 (ACED01000008). The ORF labeled with an asterisk does not appear in the Y412MC61 genome database.

ACKNOWLEDGMENT

We are grateful to S. Valla for the gift of pPR9TT.

REFERENCES

1. **Abe, T., E. Masai, K. Miyauchi, Y. Katayama, and M. Fukuda.** 2005. A tetrahydrofolate-dependent *O*-demethylase, LigM, is crucial for catabolism of vanillate and syringate in *Sphingomonas paucimobilis* SYK-6. J. Bacteriol. **187:**2030–2037.
2. **Arias-Barrau, E., E. R. Olivera, J. M. Luengo, C. Fernández, B. Galán, J. L. García, E. Díaz, and B. Miñambres.** 2004. The homogentisate pathway: a central catabolic pathway involved in the degradation of L-phenylalanine, L-tyrosine, and 3-hydroxyphenylacetate in *Pseudomonas putida*. J. Bacteriol. **186:**5062–5077.
3. **Asturias, J. A., L. D. Eltis, M. Prucha, and K. N. Timmis.** 1994. Analysis of three 2,3-dihydroxybiphenyl 1,2-dioxygenases found in *Rhodococcus globerulus* P6. Identification of a new family of extradiol dioxygenases. J. Biol. Chem. **269:**7807–7815.
4. **Bartilson, M., and V. Shingler.** 1989. Nucleotide sequence and expression of the catechol 2,3-dioxygenase-encoding gene of phenol-catabolizing *Pseudomonas* CF600. Gene **85:**233–238.

5. **Bradford, M. M.** 1976. A rapid and sensitive method for the quantitation of microgram quantities of protein utilizing the principle of protein-dye binding. Anal. Biochem. **72:**248–254.
6. **Cole, J. R., B. Chai, R. J. Farris, Q. Wang, S. A. Kulam, D. M. McGarrell, G. M. Garrity, and J. M. Tiedje.** 2005. The Ribosomal Database Project (RDP-II): sequences and tools for high-throughput rRNA analysis. Nucleic Acids Res. **33:**D294–D296.
7. **Crawford, R. L.** 1975. Novel pathway for degradation of protocatechuic acid in *Bacillus* species. J. Bacteriol. **121:**531–536.
8. **Crawford, R. L.** 1976. Pathways of 4-hydroxybenzoate degradation among species of *Bacillus*. J. Bacteriol. **127:**204–210.
9. **Crawford, R. L., J. W. Bromley, and P. E. Perkins-Olson.** 1979. Catabolism of protocatechuate by *Bacillus macerans*. Appl. Environ. Microbiol. **37:**614–618.
10. **Dal, S., G. Trautwein, and U. Gerischer.** 2005. Transcriptional organization of genes for protocatechuate and quinate degradation from *Acinetobacter* sp. strain ADP1. Appl. Environ. Microbiol. **71:**1025–1034.
11. **DiMarco, A. A., B. Averhoff, and L. N. Ornston.** 1993. Identification of the transcriptional activator *pobR* and characterization of its role in the expression of *pobA*, the structural gene for *p*-hydroxybenzoate hydroxylase in *Acinetobacter calcoaceticus*. J. Bacteriol. **175:**4499–4506.
12. **Dunwell, J. M., A. Culham, C. E. Carter, C. R. Sosa-Aguirre, and P. W. Goodenough.** 2001. Evolution of functional diversity in the cupin superfamily. Trends Biochem. Sci. **26:**740–746.
13. **Eaton, R. W.** 2001. Plasmid-encoded phthalate catabolic pathway in *Arthrobacter keyseri* 12B. J. Bacteriol. **183:**3689–3703.
14. **Eltis, L. D., and J. T. Bolin.** 1996. Evolutionary relationships among extradiol dioxygenases. J. Bacteriol. **178:**5930–5937.
15. **Eppink, M. H., K. M. Overkamp, H. A. Schreuder, and W. J. Van Berkel.** 1999. Switch of coenzyme specificity of *p*-hydroxybenzoate hydroxylase. J. Mol. Biol. **292:**87–96.
16. **Eppink, M. H., H. A. Schreuder, and W. J. van Berkel.** 1998. Lys42 and Ser42 variants of *p*-hydroxybenzoate hydroxylase from *Pseudomonas fluorescens* reveal that Arg42 is essential for NADPH binding. Eur. J. Biochem. **253:**194–201.
17. **Farinha, M. A., and A. M. Kropinski.** 1990. Construction of broad-host-range plasmid vectors for easy visible selection and analysis of promoters. J. Bacteriol. **172:**3496–3499.
18. **Franklin, F. C., M. Bagdasarian, M. M. Bagdasarian, and K. N. Timmis.** 1981. Molecular and functional analysis of the TOL plasmid pWWO from *Pseudomonas putida* and cloning of genes for the entire regulated aromatic ring *meta* cleavage pathway. Proc. Natl. Acad. Sci. USA **78:**7458–7462.
19. **Fukuoka, S., K. Ishiguro, K. Yanagihara, A. Tanabe, Y. Egashira, H. Sanada, and K. Shibata.** 2002. Identification and expression of a cDNA encoding human α-amino-β-carboxymuconate-ε-semialdehyde decarboxylase (ACMSD). A key enzyme for the tryptophan-niacine pathway and "quinolinate hypothesis". J. Biol. Chem. **277:**35162–35167.
20. **Gerischer, U., A. Segura, and L. N. Ornston.** 1998. PcaU, a transcriptional activator of genes for protocatechuate utilization in *Acinetobacter*. J. Bacteriol. **180:**1512–1524.
21. **Hanahan, D.** 1983. Studies on transformation of *Escherichia coli* with plasmids. J. Mol. Biol. **166:**557–580.
22. **Hara, H., E. Masai, Y. Katayama, and M. Fukuda.** 2000. The 4-oxalomesaconate hydratase gene, involved in the protocatechuate 4,5-cleavage pathway, is essential to vanillate and syringate degradation in *Sphingomonas paucimobilis* SYK-6. J. Bacteriol. **182:**6950–6957.
23. **Harayama, S., P. R. Lehrbach, and K. N. Timmis.** 1984. Transposon mutagenesis analysis of *meta*-cleavage pathway operon genes of the TOL plasmid of *Pseudomonas putida* mt-2. J. Bacteriol. **160:**251–255.
24. **Harayama, S., and M. Rekik.** 1989. Bacterial aromatic ring-cleavage enzymes are classified into two different gene families. J. Biol. Chem. **264:**15328–15333.
25. **Harayama, S., M. Rekik, K. L. Ngai, and L. N. Ornston.** 1989. Physically associated enzymes produce and metabolize 2-hydroxy-2,4-dienoate, a chemically unstable intermediate formed in catechol metabolism via *meta* cleavage in *Pseudomonas putida*. J. Bacteriol. **171:**6251–6258.
26. **Harwood, C. S., and R. E. Parales.** 1996. The β-ketoadipate pathway and the biology of self-identity. Annu. Rev. Microbiol. **50:**553–590.
27. **Hayase, N., K. Taira, and K. Furukawa.** 1990. *Pseudomonas putida* KF715 *bphABCD* operon encoding biphenyl and polychlorinated biphenyl degradation: cloning, analysis, and expression in soil bacteria. J. Bacteriol. **172:**1160–1164.
28. **Huang, Y., K. X. Zhao, X. H. Shen, C. Y. Jiang, and S. J. Liu.** 2008. Genetic and biochemical characterization of a 4-hydroxybenzoate hydroxylase from *Corynebacterium glutamicum*. Appl. Microbiol. Biotechnol. **78:**75–83.
29. **Kasai, D., E. Masai, K. Miyauchi, Y. Katayama, and M. Fukuda.** 2004. Characterization of the 3-*O*-methylgallate dioxygenase gene and evidence of multiple 3-*O*-methylgallate catabolic pathways in *Sphingomonas paucimobilis* SYK-6. J. Bacteriol. **186:**4951–4959.
30. **Kasai, D., E. Masai, K. Miyauchi, Y. Katayama, and M. Fukuda.** 2005. Characterization of the gallate dioxygenase gene: three distinct ring cleavage dioxygenases are involved in syringate degradation by *Sphingomonas paucimobilis* SYK-6. J. Bacteriol. **187:**5067–5074.
31. **Koehntop, K. D., J. P. Emerson, and L. Que, Jr.** 2005. The 2-His-1-carboxylate facial triad: a versatile platform for dioxygen activation by mononuclear non-heme iron(II) enzymes. J. Biol. Inorg. Chem. **10:**87–93.
32. **Li, T., H. Iwaki, R. Fu, Y. Hasegawa, H. Zhang, and A. Liu.** 2006. α-Amino-β-carboxymuconic-ε-semialdehyde decarboxylase (ACMSD) is a new member of the amidohydrolase superfamily. Biochemistry **45:**6628–6634.
33. **Liu, A., and H. Zhang.** 2006. Transition metal-catalyzed nonoxidative decarboxylation reactions. Biochemistry **45:**10407–10411.
34. **Martynowski, D., Y. Eyobo, T. Li, K. Yang, A. Liu, and H. Zhang.** 2006. Crystal structure of α-amino-β-carboxymuconate-ε-semialdehyde decarboxylase: insight into the active site and catalytic mechanism of a novel decarboxylation reaction. Biochemistry **45:**10412–10421.
35. **Maruyama, K., T. Shibayama, A. Ichikawa, Y. Sakou, S. Yamada, and H. Sugisaki.** 2004. Cloning and characterization of the genes encoding enzymes for the protocatechuate *meta*-degradation pathway of *Pseudomonas ochraceae* NGJ1. Biosci. Biotechnol. Biochem. **68:**1434–1441.
36. **Masai, E., Y. Katayama, and M. Fukuda.** 2007. Genetic and biochemical investigations on bacterial catabolic pathways for lignin-derived aromatic compounds. Biosci. Biotechnol. Biochem. **71:**1–15.
37. **Masai, E., K. Momose, H. Hara, S. Nishikawa, Y. Katayama, and M. Fukuda.** 2000. Genetic and biochemical characterization of 4-carboxy-2-hydroxymuconate-6-semialdehyde dehydrogenase and its role in the protocatechuate 4,5-cleavage pathway in *Sphingomonas paucimobilis* SYK-6. J. Bacteriol. **182:**6651–6658.
38. **Miller, J. H.** 1972. Experiments in molecular genetics. Cold Spring Harbor Laboratory, Cold Spring Harbor, NY.
39. **Muraki, T., M. Taki, Y. Hasegawa, H. Iwaki, and P. C. Lau.** 2003. Prokaryotic homologs of the eukaryotic 3-hydroxyanthranilate 3,4-dioxygenase and 2-amino-3-carboxymuconate-6-semialdehyde decarboxylase in the 2-nitrobenzoate degradation pathway of *Pseudomonas fluorescens* strain KU-7. Appl. Environ. Microbiol. **69:**1564–1572.
40. **Nakai, C., H. Kagamiyama, M. Nozaki, T. Nakazawa, S. Inouye, Y. Ebina, and A. Nakazawa.** 1983. Complete nucleotide sequence of the metapyrocatechase gene on the TOL plasmid of *Pseudomonas putida* mt-2. J. Biol. Chem. **258:**2923–2928.
41. **Noda, Y., S. Nishikawa, K. Shiozuka, H. Kadokura, H. Nakajima, K. Yoda, Y. Katayama, N. Morohoshi, T. Haraguchi, and M. Yamasaki.** 1990. Molecular cloning of the protocatechuate 4,5-dioxygenase genes of *Pseudomonas paucimobilis*. J. Bacteriol. **172:**2704–2709.
42. **Nogales, J., Á. Canales, J. Jiménez-Barbero, J. L. García, and E. Díaz.** 2005. Molecular characterization of the gallate dioxygenase from *Pseudomonas putida* KT2440. The prototype of a new subgroup of extradiol dioxygenases. J. Biol. Chem. **280:**35382–35390.
43. **Nordlund, I., and V. Shingler.** 1990. Nucleotide sequences of the *meta*-cleavage pathway enzymes 2-hydroxymuconic semialdehyde dehydrogenase and 2-hydroxymuconic semialdehyde hydrolase from *Pseudomonas* CF600. Biochim. Biophys. Acta **1049:**227–230.
44. **Peng, X., T. Egashira, K. Hanashiro, E. Masai, S. Nishikawa, Y. Katayama, K. Kimbara, and M. Fukuda.** 1998. Cloning of a *Sphingomonas paucimobilis* SYK-6 gene encoding a novel oxygenase that cleaves lignin-related biphenyl and characterization of the enzyme. Appl. Environ. Microbiol. **64:**2520–2527.
45. **Peng, X., E. Masai, Y. Katayama, and M. Fukuda.** 1999. Characterization of the *meta*-cleavage compound hydrolase gene involved in degradation of the lignin-related biphenyl structure by *Sphingomonas paucimobilis* SYK-6. Appl. Environ. Microbiol. **65:**2789–2793.
46. **Peng, X., E. Masai, H. Kitayama, K. Harada, Y. Katayama, and M. Fukuda.** 2002. Characterization of the 5-carboxyvanillate decarboxylase gene and its role in lignin-related biphenyl catabolism in *Sphingomonas paucimobilis* SYK-6. Appl. Environ. Microbiol. **68:**4407–4415.
47. **Providenti, M. A., J. Mampel, S. MacSween, A. M. Cook, and R. C. Wyndham.** 2001. *Comamonas testosteroni* BR6020 possesses a single genetic locus for extradiol cleavage of protocatechuate. Microbiology **147:**2157–2167.
48. **Romero-Steiner, S., R. E. Parales, C. S. Harwood, and J. E. Houghton.** 1994. Characterization of the *pcaR* regulatory gene from *Pseudomonas putida*, which is required for the complete degradation of *p*-hydroxybenzoate. J. Bacteriol. **176:**5771–5779.
49. **Roper, D. I., and R. A. Cooper.** 1990. Subcloning and nucleotide sequence of the 3,4-dihydroxyphenylacetate (homoprotocatechuate) 2,3-dioxygenase gene from *Escherichia coli* C. FEBS Lett. **275:**53–57.
50. **Saito, I., and G. R. Stark.** 1986. Charomids: cosmid vectors for efficient cloning and mapping of large or small restriction fragments. Proc. Natl. Acad. Sci. USA **83:**8664–8668.
51. **Saitou, N., and M. Nei.** 1987. The neighbor-joining method: a new method for reconstructing phylogenetic trees. Mol. Biol. Evol. **4:**406–425.
52. **Sala-Trepat, J. M., and W. C. Evans.** 1971. The *meta* cleavage of catechol by *Azotobacter* species. 4-Oxalocrotonate pathway. Eur. J. Biochem. **20:**400–413.
53. **Santos, P. M., I. Di Bartolo, J. M. Blatny, E. Zennaro, and S. Valla.** 2001.

New broad-host-range promoter probe vectors based on the plasmid RK2 replicon. FEMS Microbiol. Lett. **195:**91–96.

54. **Sasoh, M., E. Masai, S. Ishibashi, H. Hara, N. Kamimura, K. Miyauchi, and M. Fukuda.** 2006. Characterization of the terephthalate degradation genes of *Comamonas* sp. strain E6. Appl. Environ. Microbiol. **72:**1825–1832.
55. **Shingler, V., J. Powlowski, and U. Marklund.** 1992. Nucleotide sequence and functional analysis of the complete phenol/3,4-dimethylphenol catabolic pathway of *Pseudomonas* sp. strain CF600. J. Bacteriol. **174:**711–724.
56. **Short, J. M., J. M. Fernandez, J. A. Sorge, and W. D. Huse.** 1988. λ ZAP: a bacteriophage λ expression vector with *in vivo* excision properties. Nucleic Acids Res. **16:**7583–7600.
57. **Smiley, J. A., M. Kundracik, D. A. Landfried, V. R. Barnes, Sr., and A. A. Axhemi.** 2005. Genes of the thymidine salvage pathway: thymine-7-hydroxylase from a *Rhodotorula glutinis* cDNA library and *iso*-orotate decarboxylase from *Neurospora crassa*. Biochim. Biophys. Acta **1723:**256–264.
58. **Sota, M., H. Yano, A. Ono, R. Miyazaki, H. Ishii, H. Genka, E. M. Top, and M. Tsuda.** 2006. Genomic and functional analysis of the IncP-9 naphthalene-catabolic plasmid NAH7 and its transposon Tn*4655* suggests catabolic gene spread by a tyrosine recombinase. J. Bacteriol. **188:**4057–4067.
59. **Studier, F. W., and B. A. Moffatt.** 1986. Use of bacteriophage T7 RNA polymerase to direct selective high-level expression of cloned genes. J. Mol. Biol. **189:**113–130.
60. **Sugimoto, K., T. Senda, H. Aoshima, E. Masai, M. Fukuda, and Y. Mitsui.** 1999. Crystal structure of an aromatic ring opening dioxygenase LigAB, a protocatechuate 4,5-dioxygenase, under aerobic conditions. Structure Fold. Des. **7:**953–965.
61. **Takenaka, S., S. Murakami, R. Shinke, K. Hatakeyama, H. Yukawa, and K. Aoki.** 1997. Novel genes encoding 2-aminophenol 1,6-dioxygenase from *Pseudomonas* species AP-3 growing on 2-aminophenol and catalytic properties of the purified enzyme. J. Biol. Chem. **272:**14727–14732.
62. **Tanabe, A., Y. Egashira, S. Fukuoka, K. Shibata, and H. Sanada.** 2002. Purification and molecular cloning of rat 2-amino-3-carboxymuconate-6-semialdehyde decarboxylase. Biochem. J. **361:**567–575.
63. **Vaillancourt, F. H., J. T. Bolin, and L. D. Eltis.** 2006. The ins and outs of ring-cleaving dioxygenases. Crit. Rev. Biochem. Mol. Biol. **41:**241–267.
64. **Wolgel, S. A., J. E. Dege, P. E. Perkins-Olson, C. H. Jaurez-Garcia, R. L. Crawford, E. Münck, and J. D. Lipscomb.** 1993. Purification and characterization of protocatechuate 2,3-dioxygenase from *Bacillus macerans*: a new extradiol catecholic dioxygenase. J. Bacteriol. **175:**4414–4426.
65. **Yanisch-Perron, C., J. Vieira, and J. Messing.** 1985. Improved M13 phage cloning vectors and host strains: nucleotide sequences of the M13mp18 and pUC19 vectors. Gene **33:**103–119.
66. **Yoshida, M., N. Fukuhara, and T. Oikawa.** 2004. Thermophilic, reversible γ-resorcylate decarboxylase from *Rhizobium* sp. strain MTP-10005: purification, molecular characterization, and expression. J. Bacteriol. **186:**6855–6863.
67. **Yoshida, M., T. Oikawa, H. Obata, K. Abe, H. Mihara, and N. Esaki.** 2007. Biochemical and genetic analysis of the γ-resorcylate (2,6-dihydroxybenzoate) catabolic pathway in *Rhizobium* sp. strain MTP-10005: identification and functional analysis of its gene cluster. J. Bacteriol. **189:**1573–1581.